Mesoscale Modeling of Katabatic Winds over Greenland with the Polar MM5*

DAVID H. BROMWICH

Polar Meteorology Group, Byrd Polar Research Center, and Atmospheric Sciences Program, Department of Geography, The Ohio State University, Columbus, Ohio

JOHN J. CASSANO

Polar Meteorology Group, Byrd Polar Research Center, The Ohio State University, Columbus, Ohio

THOMAS KLEIN AND GUNTHER HEINEMANN

Meteorologisches Institut der Universitat Bonn, Bonn, Germany

KEITH M. HINES

Polar Meteorology Group, Byrd Polar Research Center, The Ohio State University, Columbus, Ohio

KONRAD STEFFEN AND JASON E. BOX

Cooperative Institute for Research in Environmental Sciences, University of Colorado, Boulder, Colorado

(Manuscript received 5 April 2000, in final form 16 February 2001)

ABSTRACT

Verification of two months, April and May 1997, of 48-h mesoscale model simulations of the atmospheric state around Greenland are presented. The simulations are performed with a modified version of The Pennsylvania State University–National Center for Atmospheric Research fifth-generation Mesoscale Model (MM5), referred to as the Polar MM5. Global atmospheric analyses as well as automatic weather station and instrumented aircraft observations from Greenland are used to verify the forecast atmospheric state. The model is found to reproduce the observed atmospheric state with a high degree of realism. Monthly mean values of the near-surface temperature and wind speed predicted by the Polar MM5 differ from the observations by less than 1 K and 1 m s^{-1}, respectively, at most sites considered. In addition, the model is able to simulate a realistic diurnal cycle for the surface variables, as well as capturing the large-scale, synoptically forced changes in these variables. Comparisons of modeled profiles of wind speed, direction, and potential temperature in the katabatic layer with aircraft observations are also favorable, with small mean errors. The simulations of the katabatic winds are found to be sensitive to errors in the large-scale forcing (e.g., the large-scale pressure gradient) and to errors in the representation of key physical processes, such as turbulence in the very stable surface layer and cloud–radiation interaction.

1. Introduction

Numerical simulations of katabatic winds over the Antarctic and Greenland ice sheets have been presented in the refereed literature beginning with the work of Parish (1984). Many of the katabatic wind simulations presented in the literature have used two- and three-dimensional, numerical models with idealized large-scale atmospheric forcing (e.g., Parish 1984; Pettré et al. 1990; Gallée and Schayes 1992; Bromwich et al. 1994; Bromwich et al. 1996; Gallée and Duynkerke 1997; Heinemann 1997). More recent publications have described three-dimensional simulations of katabatic winds forced by realistic atmospheric conditions (Hines et al. 1995; Walsh and McGregor 1996; Hines et al. 1997a,b; van Lipzig et al. 1999). In both cases, the verification of these simulations is often limited to global atmospheric analyses, widely spaced automatic weather station (AWS) observations, or data from a single site of a field campaign. Results from these studies have indicated serious problems in the representation of clouds, radiation, and turbulent processes near the surface.

Increased research into processes acting in the polar

* Byrd Polar Research Center Contribution Number 1149.

Corresponding author address: John Cassano, CIRES, Campus Box 216, University of Colorado, Boulder, CO 80309-0216.
E-mail: cassano@terra.colorado.edu

atmosphere, through observational campaigns such as SHEBA (Pinto et al. 1999), GIMEX (Oerlemans and Vugts 1993), and the FIRE Arctic Clouds Experiment (Curry et al. 2000), has allowed for refinement of the numerical models used for simulations in this environment. In particular improvements in the understanding of cloud and radiation processes have provided for potentially dramatic improvements in the skill of mesoscale model simulations of the near-surface atmospheric state over large ice sheets.

Based on the experience of previous research into mesoscale modeling in polar regions, The Pennsylvania State University–National Center for Atmospheric Research (PSU–NCAR) fifth-generation Mesoscale Model (MM5) has been modified for use in polar regions (referred to as the Polar MM5). The Polar MM5 modifications described in this paper are now available in the public release version of MM5 (v3.5 and later).

The results of two months (April and May 1997) of 48-h simulations of the katabatic winds over Greenland using the Polar MM5 are presented in this paper. The model verification results for this two-month period are presented to illustrate the potential skill of the Polar MM5 over extensive ice sheets. Sensitivity simulations are presented to illustrate potential sources of errors in some of the katabatic wind simulations.

Data used for verification of the Polar MM5 simulations include operational global atmospheric analyses from the European Centre for Medium-Range Weather Forecasts (ECMWF), AWS observations from sites on the Greenland ice sheet (Steffen et al. 1996; Heinemann 1999), and instrumented aircraft observations of the katabatic layer over Greenland obtained during the Katabatic Wind and Boundary Layer Front Experiment around Greenland during 1997 (KABEG'97) (Heinemann 1999). A more detailed description of the data used to verify the Polar MM5 simulations is given in section 2.

Section 3 of this paper describes the Polar MM5 and the changes made to this model for use in polar regions. Descriptions of the model configuration, initialization, and forecast procedure used for this study are also presented in this section. The model verification results are described in section 4, with emphasis given to the AWS and instrumented aircraft observations. Concluding remarks are presented in section 5.

2. Observational data used for model verification

The primary observational data used for verification of the Polar MM5 simulations presented in this paper are aircraft and AWS observations from the KABEG'97 field campaign and AWS observations from the Greenland Climate Network (GC-NET) AWS array.

The aircraft data collected during KABEG'97 include the aircraft position, wind components, air temperature, and humidity sampled at rates of 12–120 Hz [additional details on the aircraft measurements can be found in Heinemann (1999)]. The aircraft data used in this study are ''vertical'' profiles observed as the aircraft performed slantwise ascents (or descents) to a height of 400 m above ground level (AGL). The aircraft profiles are measured over a horizontal distance of approximately 5 km. A list of the aircraft profiles used for model verification in this paper is given in Table 1. The location of the aircraft profiles are shown in Figs. 1b,c (locations A4, I4, and P4). AWS observations from site A4 (Figs. 1b,c) are used for model verification from 16 April to 17 May 1997.

TABLE 1. List of katabatic wind flights during the KABEG '97 field program with the date/time (UTC) and location of aircraft profiles used for model verification.

Flight number	Date/time	Location
KA1	18 Apr 1997/0740	A4
KA2	21 Apr 1997/0710	A4
KA3	22 Apr 1997/0740	A4
KA4	29 Apr 1997/1100	A4
KA5	2 May 1997/0640	A4
KA6	11 May 1997/0810	P4
KA8	13 May 1997/0630	A4
KA9	14 May 1997/0710	I4

During April and May 1997 13 AWSs were operating as part of the GC-NET AWS array. A description of the GC-NET AWS measurements and site locations is given by Steffen et al. (1996). Observations from six of the GC-NET AWSs operating during April and May 1997 are used to verify the Polar MM5 (Table 2, Fig. 1b). These six sites are selected for model verification purposes since they contain a nearly complete record of observations during the two-month period of interest and because they provide observations of the near-surface atmospheric state over a large area of the Greenland ice sheet. Model verification results from the remaining seven GC-NET AWS sites are not presented, but they are similar to the results described in section 4b.

3. Description of the Polar MM5

The Polar MM5 model used for the simulations presented in this paper is based on version 2 of the PSU–NCAR MM5. A general description of this model is given by Dudhia (1993) and Grell et al. (1994). The model configuration used for the simulations presented in this paper is described below. In addition, a description of the changes made to the standard version of MM5 for use in polar regions is provided.

a. Polar MM5 dynamics and physics

The standard version of MM5 (version 2) allows for the use of either hydrostatic or nonhydrostatic governing dynamics. For the Greenland simulations presented in this paper the hydrostatic dynamics option is used since the hydrostatic approximation is valid for the model

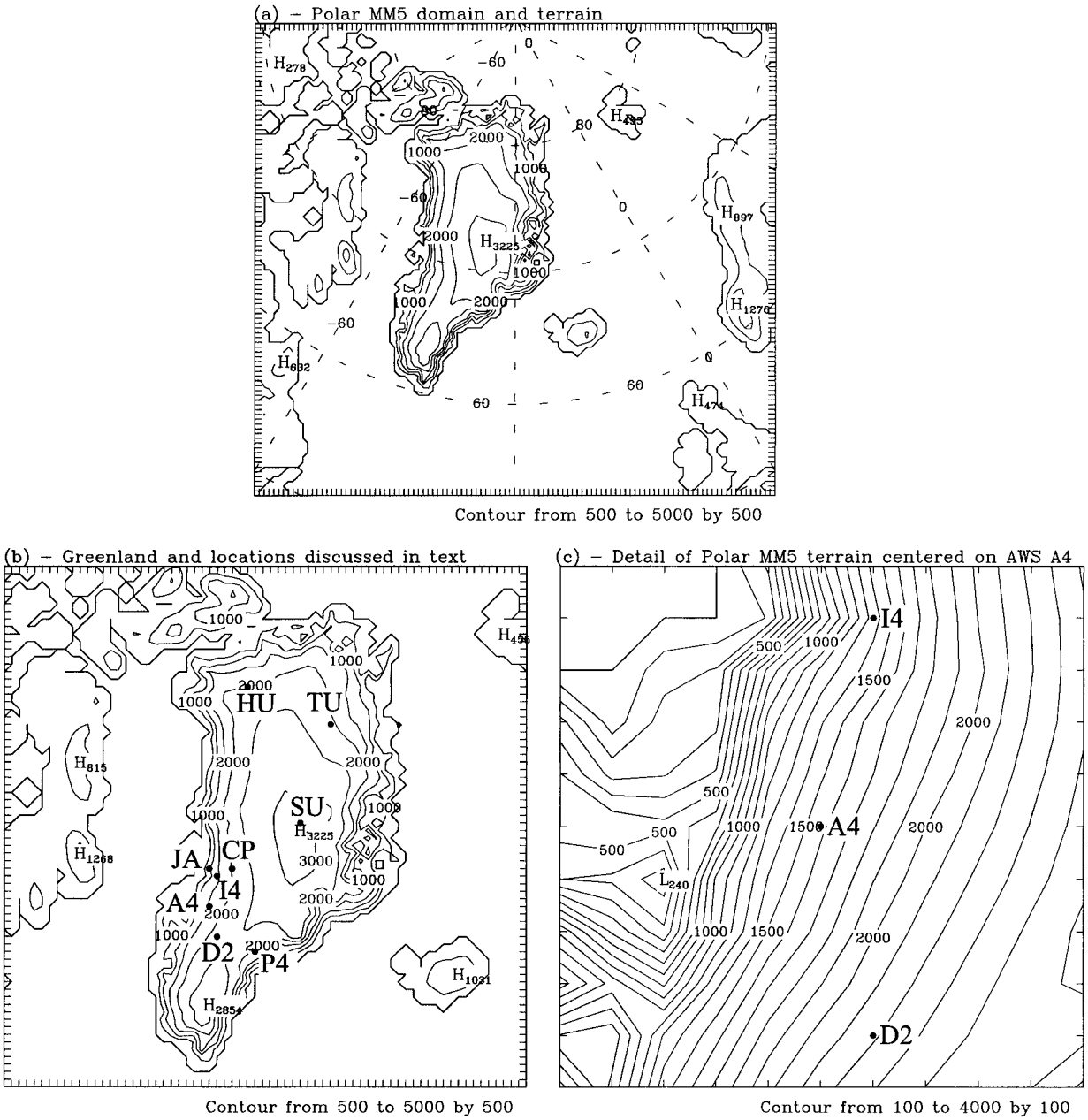

FIG. 1. (a) Map of Polar MM5 model domain, with terrain elevation contours (solid lines, 500-m contour interval), zero elevation contour (bold line), and latitude (dashed lines, 10° contour interval) and longitude (dashed lines, 30° contour interval); (b) detail of Polar MM5 model domain centered on Greenland, with terrain elevation contours (solid lines, 500-m contour interval), zero elevation contour (bold line), and locations of sites discussed in text marked with filled circles (HU: Humboldt AWS, TU: Tunu-N AWS, SU: Summit AWS, JA: JAR 1 AWS, CP: Crawford Point AWS, A4: KABEG AWS A4, D2: Dye-2 AWS, and I4 and P4: location of aircraft profiles); and (c) detail of Polar MM5 model domain centered on KABEG AWS A4, with terrain elevation contours (solid lines, 100-m contour interval), zero elevation contour (bold line), and location of sites I4, A4, and D2 marked with filled circles. Tick marks on borders of each panel indicate spacing of model grid points (40 km).

horizontal resolution used (40 km), and the hydrostatic option was found to run approximately 12% faster than the nonhydrostatic option. The hydrostatic version of the model includes three-dimensional prognostic equations for the horizontal components of the wind and temperature, and a two-dimensional prognostic equation for p^* (defined as the surface pressure minus the pressure at the model top). Additional three-dimensional prognostic equations for the water vapor mixing ratio and the mixing ratio of various cloud species are also part of the model equations. Parameterizations for cloud microphysics and precipitation processes, cumulus con-

TABLE 2. List of GC-NET AWSs used for model verification during Apr and May 1997.

Station name	Latitude (°N)	Longitude (°W)	Elevation (m)
Humboldt	78.53	56.83	1995*
Tunu-N	78.02	33.99	2113*
Summit	72.58	38.50	3254
Crawford Point	69.88	46.99	2022
JAR1	69.50	49.68	962*
Dye-2	66.48	46.28	2165

* Elevation of AWS determined with differential GPS measurements.

vection, radiative transfer, and turbulence are included in the model, with multiple options available for the representation of many of these processes.

For the Polar MM5 simulations the large-scale (grid scale) cloud and precipitation processes are represented by the Reisner explicit microphysics parameterization (Reisner et al. 1998). This parameterization predicts the mixing ratio of cloud water and ice crystals as well as the rain and snow water mixing ratios, and allows for the presence of mixed phase clouds. Subgrid-scale clouds are parameterized with the Grell cumulus parameterization (Grell et al. 1994).

Excessive cloud cover was found to be a problem over the Antarctic in sensitivity simulations using an older version of MM5 (MM4) (Hines et al. 1997a,b), similar to results found by Manning and Davis (1997) for cold, high clouds over the continental United States. Replacement of the Fletcher (1962) equation for ice nuclei concentration with that of Meyers et al. (1992) in the MM5 explicit microphysics parameterizations, as suggested by Manning and Davis (1997), helped to eliminate this cloudy bias in polar simulations with MM5, and is now a standard option in the Polar MM5 model. This modification to the Reisner microphysics parameterization is used for all of the simulations presented here.

The Polar MM5 also uses a modified version of the NCAR community climate model, version 2 (CCM2), radiation parameterization (Hack et al. 1993) for prediction of the radiative transfer of shortwave and longwave radiation through the atmosphere. In the original version of this parameterization the cloud cover was predicted as a simple function of the grid-box relative humidity, with the cloud liquid water (CLW) path determined from the grid-box temperature. Sensitivity simulations revealed that this parameterization of cloud cover tended to significantly overestimate the CLW path, and thus the radiative effects of the clouds, which was particularly noticeable as large downwelling longwave radiation fluxes during the austral winter over the Antarctic ice sheet (Hines et al. 1997a,b). In order to resolve this problem, the predicted cloud water and ice mixing ratios from the Reisner explicit microphysics parameterization are used in the modified CCM2 radiation parameterization for determination of the radiative properties of the modeled cloud cover. This modification allows for a consistent treatment of the radiative and microphysical properties of the clouds and for the separate treatment of the radiative properties of liquid and ice phase cloud particles, similar to that in the CCM3 radiation parameterization (Kiehl et al. 1996) that is in part based on results discussed by Ebert and Curry (1992).

Turbulent fluxes in the atmosphere, and the turbulent fluxes between the atmosphere and the surface, are parameterized using the 1.5-order turbulence closure parameterization used in the National Centers for Environmental Prediction Eta Model (Janjić 1994). Heat transfer through the model substrate is predicted using a multilayer ''soil'' model. The thermal properties used in the soil model for snow and ice surface types are modified following Yen (1981). In addition, the number of substrate levels represented in the soil model was increased from six to eight, with an increase in the resolved substrate depth from 0.47 m to 1.91 m. Also, a sea ice surface type is added to the 13 surface types available in the standard version of MM5 (Hines et al. 1997a). The sea ice surface type allows for fractional sea ice cover in any oceanic grid point, with surface fluxes for the sea ice grid points calculated separately for the open water and sea ice portions of the grid point, which are then averaged before interacting with the overlying atmosphere. The sea ice thickness varies from 0.2 m to 0.95 m and is dependent on the hemisphere and sea ice fraction at the grid point (Table 3). Some surface characteristics for the surface types of interest in this study are listed in Table 3.

b. Model grid

MM5 is formulated using a staggered horizontal grid with a vertical σ-coordinate system that is defined in terms of pressure. The model domain used in this study consists of 100 grid points in the north–south direction and 110 grid points in the east–west direction, centered at 71°N latitude and 30°W longitude, with a horizontal resolution of 40 km (Fig. 1). The model terrain over Greenland is specified from the Ekholm (1996) digital elevation data (Table 3), since accurate representation of the terrain slope over the ice sheet is required for accurate katabatic wind simulations. The 40-km horizontal grid spacing used in the Polar MM5 adequately resolves the terrain slopes over all but the steepest margins of the ice sheet (Cassano and Parish 2000).

A total of 28 σ levels are used, of which seven are located within the lowest 400 m of the atmosphere, and the lowest atmospheric model level is located at a nominal height of 12 m AGL. This relatively high resolution near the surface is required to accurately represent the evolution of the shallow katabatic layer over the Greenland ice sheet. The model top is set at a constant pressure of 100 hPa.

TABLE 3. List of surface characteristics and input data used for Polar MM5 simulations.

Surface characteristics		
Surface type	Albedo	Roughness length (m)
Ice sheet	0.80	1×10^{-4}
Tundra (summer)	0.15	0.1
Tundra (winter)	0.70	0.1
Sea ice	0.70	1×10^{-3}
Ocean	0.15	minimum 1×10^{-4} with Charnock relation

Input data	
Initial and boundary condition atmospheric data	12 hourly 2.5° ECMWF TOGA global analyses
Topography	Ekholm (1996), 2-km resolution
Sea surface temperature	6-hourly 1.125° ECMWF TOGA global surface analyses
Sea ice coverage	Sea ice surface type for ocean grid points with SST $<$ 271.7 K, sea ice fraction based on climatological values (Gloersen et al. 1992)
Sea ice thickness*:	
NH, conc. $\geq$ 0.9	0.95 m
NH, 0.6 $\leq$ conc. $<$ 0.9	0.47 m
NH, conc. $<$ 0.6	0.23 m
SH, all conc.	0.23 m

* NH: Northern Hemisphere; SH: Southern Hemisphere, conc.: sea ice concentration in grid cell.

c. Polar MM5 initial and boundary condition data

A list of the datasets used to initialize the Polar MM5, and those that are used to provide boundary conditions to the model during the simulations, are listed in Table 3. The 2.5° horizontal resolution ECMWF Tropical Ocean Global Atmosphere (TOGA) surface and upper-air data are used to provide the initial and boundary conditions for the model atmosphere. These data are interpolated to the Polar MM5 model grid using the standard preprocessing programs provided by NCAR for use with the MM5 modeling system. In addition the 1.125° ECMWF TOGA global surface analyses are used to specify the initial surface temperature [and sea surface temperature (SST)], deep soil temperature, and snow cover. Snow cover on the tundra grid points on Greenland is manually specified to match snow cover observations from the KABEG'97 field campaign. Sea ice cover is based on the SST specified with the higher-resolution surface data, and is considered to be present at all grid points with an SST $<$ 271.7 K. Sea ice fraction for these grid points is determined based on climatological values given by Gloersen et al. (1992).

The Polar MM5 was used to produce short duration (48-h length) simulations of the atmospheric state over Greenland for April and May 1997. The model was initialized with the 0000 UTC ECMWF analyses for each day of the two-month period, with the 24–48-h forecast used for model verification, unless otherwise noted.

4. Validation of Polar MM5

The Polar MM5 forecasts are compared to three datasets for the purpose of model verification, including the global 2.5° ECMWF TOGA global analyses, AWS observations, and aircraft data collected during the KABEG'97 field campaign.

a. Verification of the Polar MM5 forecasts with ECMWF analyses

The 2.5° ECMWF analyses were used to verify the large-scale atmospheric features simulated by the Polar MM5. Figure 2 displays vertical profiles of the spatial and temporal mean difference (bias) between selected Polar MM5 and ECMWF analysis fields. The ECMWF analyses (on constant pressure levels at 1000, 850, 700, 500, 400, 300, 250, 200, 150, and 100 hPa) are interpolated to the Polar MM5 model grid and compared to the 24- and 36-h forecasts from the Polar MM5. The bias is calculated for the entire model domain, all oceanic grid points, and grid points over the Greenland ice sheet (with the five grid points closest to the model domain lateral boundaries excluded from the calculation for each of these areas, since these grid points are directly influenced by the imposed lateral boundary conditions). The vertical profiles are plotted as a function of the model σ levels, with a pressure scale calculated for grid points with a surface pressure of 1000 hPa plotted for reference.

For all regions of the model domain considered the magnitude of the bias in the temperature field is less than 1 K, except near the surface and for $\sigma < 0.2$ (Figs. 2a and 2b). Over Greenland the model has a tendency to simulate cooler temperatures near the surface and warmer temperatures aloft compared to the ECMWF analyses. This indicates that the Polar MM5 simulates a stronger low-level temperature inversion than is pre-

→

FIG. 2. Profiles of the monthly mean bias of temperature [(a) and (b)], water vapor mixing ratio [(c) and (d)], zonal wind speed [(e) and (f)], and meridional wind speed [(g) and (h)], calculated as the difference between the monthly mean Polar MM5 predicted values and values from the 2.5° resolution ECMWF global analyses (Polar MM5 − ECMWF), plotted as a function of the model sigma levels (vertical scale on left side of graphs). The pressure is plotted on the vertical scale on the right side of the graphs, for grid points with a surface pressure of 1000 hPa. Biases for Apr 1997 are plotted in (a), (c), (e), and (g) and biases for May 1997 are plotted in (b), (d), (f), and (h). Biases are area averaged over the entire model domain (thin, solid line), over all oceanic grid points (thin, dashed line), and over all permanent ice grid points over Greenland (thick, solid line) (with the five grid points closest to the model domain lateral boundaries excluded from all calculations).

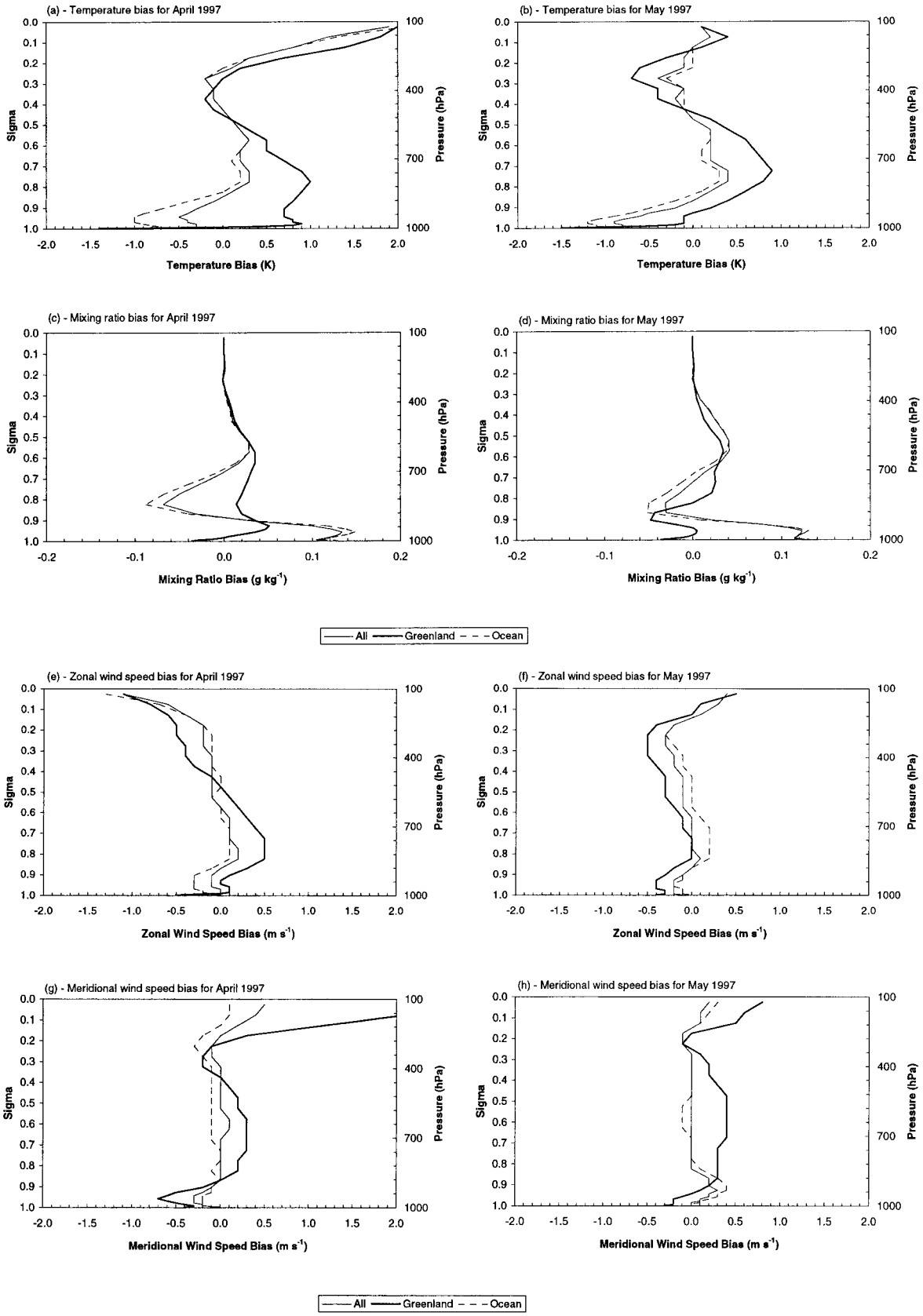
(a) - Temperature bias for April 1997
(b) - Temperature bias for May 1997
(c) - Mixing ratio bias for April 1997
(d) - Mixing ratio bias for May 1997
(e) - Zonal wind speed bias for April 1997
(f) - Zonal wind speed bias for May 1997
(g) - Meridional wind speed bias for April 1997
(h) - Meridional wind speed bias for May 1997
Sigma
Pressure (hPa)
Temperature Bias (K)
Mixing Ratio Bias (g kg-1)
Zonal Wind Speed Bias (m s-1)
Meridional Wind Speed Bias (m s-1)
All
Greenland
Ocean

TABLE 4. Statistics from the comparison of the Polar MM5 simulations to the GC-NET AWS data for Apr 1997. Statistics listed in the table include the mean of the AWS data (mean), monthly mean Polar MM5 − monthly mean AWS (bias), the root-mean-square error (rmse), and the correlation coefficient between the Polar MM5 and AWS data (corr). Maximum absolute values are printed in bold and minimum absolute values are underlined for the bias, rmse, and correlation coefficient for each variable. Variables listed include the surface pressure, near-surface air temperature, water vapor mixing ratio, wind speed, and resultant wind direction.

	Surface pressure				Temperature				Water vapor mixing ratio			
Station	Mean (hPa)	Bias (hPa)	Rmse (hPa)	Corr	Mean (K)	Bias (K)	Rmse (K)	Corr	Mean (g kg^{-1})	Bias (g kg^{-1})	Rmse (g kg^{-1})	Corr
Humboldt	780	2.33	1.89	0.98	−31.7	0.46	2.93	0.94	0.32	0.01	0.11	0.92
Tunu	777	**−5.28**	**5.99**	0.93	−31.5	−0.60	3.04	0.94	0.33	−0.02	0.13	0.86
Summit	661	2.03	2.94	0.98	−31.4	**1.34**	**4.46**	0.90	0.42	**0.09**	0.22	0.90
Crawford	783	−1.22	2.37	0.98	−23.2	−0.01	3.51	0.94				
JAR	899	−1.02	2.12	0.98	−15.8	0.77	2.56	**0.96**	1.19	0.03	**0.38**	**0.93**
Dye-2	767	1.12	2.03	**0.99**	−21.1	0.16	3.43	0.94	0.94	0.03	0.36	0.88
Average		−0.34	2.89	0.97		0.35	3.32	0.94		0.03	0.24	0.90

sent in the ECMWF analyses. In comparing the Polar MM5 modeled near-surface temperature with AWS observations from Greenland it is found that there is little systematic cold bias in the near-surface temperatures (see section 4b), and the difference between the Polar MM5 simulations and the ECMWF analyses is likely a reflection of the inadequate representation of the low-level inversion by the limited number of constant pressure levels and other errors in the ECMWF analyses. For $\sigma < 0.2$ larger biases in the temperature are found compared to lower levels, particularly for April 1997, and this is likely a result of the coarse Polar MM5 vertical grid spacing (greater than 1000 m) near the model top and the subsequent inaccurate representation of the height of the tropopause.

For the mixing ratio, the bias tends to be largest at lower levels and decreases with increasing height (Figs. 2c,d) (as a result of the decreasing magnitude of the mixing ratio with height). A positive bias greater than 0.1 g kg^{-1} is found over the ocean, and the entire model domain, at low levels ($\sigma > 0.9$). The bias is negative in the middle troposphere ($0.7 < \sigma < 0.9$), with magnitudes less than 0.1 g kg^{-1}.

The magnitude of the bias in the zonal and meridional wind components is less than 0.5 m s^{-1}, except near the model top, and is similar for all regions considered (Figs. 2e–h).

Based on this analysis it appears that the Polar MM5 simulations represent the large-scale atmospheric features depicted in the ECMWF analyses with a high degree of accuracy and minimal bias, especially in the troposphere.

b. *Verification of the Polar MM5 forecasts with AWS observations*

The near-surface forecasts from the Polar MM5 are compared to AWS observations from the Program for Arctic Regional Climate Assessment GC-NET AWS array (Steffen et al. 1996) and an AWS installed as part of the KABEG'97 field project (Heinemann 1999), using the model grid point closest to the AWS location. Statistics calculated from the comparison of the model data with the AWS observations are given in Tables 4–6. Tables 4 and 5 list the model verification statistics for the GC-NET AWS array for April and May 1997, respectively, while Table 6 lists the verification statistics for KABEG AWS A4 for 16 April–17 May 1997. The statistics listed in these tables include the mean AWS observed values, the bias (mean Polar MM5 − mean AWS), root-mean-square error (rmse), and the correlation coefficient between the observed and modeled monthly time series. Time series plots of the model predicted and AWS observed near-surface atmospheric

TABLE 5. Same as Table 4, except for May 1997.

	Surface pressure				Temperature				Water vapor mixing ratio			
Station	Mean (hPa)	Bias (hPa)	Rmse (hPa)	Corr	Mean (K)	Bias (K)	Rmse (K)	Corr	Mean (g kg^{-1})	Bias (g kg^{-1})	Rmse (g kg^{-1})	Corr
Humboldt	791	0.09	1.43	**0.99**	−17.6	1.22	2.75	0.93	1.00	0.20	0.35	0.87
Tunu	787	**−6.63**	**6.91**	0.97	−19.7	1.32	2.46	**0.95**	0.82	0.19	0.30	**0.92**
Summit	674	0.77	1.98	0.97	−24.4	**4.07**	**5.39**	0.86	0.61	**0.30**	0.40	0.77
Crawford	794	−3.43	3.79	0.98	−12.8	−0.10	2.78	0.83	1.44	0.22	0.41	0.84
JAR	906	−2.57	2.92	0.98	−4.9	0.53	2.25	0.84	2.29	0.04	**0.49**	0.79
Dye-2	778	−1.34	2.03	0.97	−11.7	−0.62	2.48	0.89	1.65	0.03	0.41	0.83
Average		−2.19	3.18	0.98		1.07	3.02	0.88		0.16	0.39	0.84

TABLE 4. (*Continued*)

Station	Wind speed: Mean (m s^{-1})	Bias (m s^{-1})	Rmse (m s^{-1})	Corr	Resultant wind direction: Mean (deg)	Bias (deg)
Humboldt	7.1	0.90	2.01	0.79	178	−5
Tunu	6.3	1.22	2.30	0.79	278	1
Summit	6.8	0.31	2.46	**0.84**	204	**−12**
Crawford	5.8	**1.59**	**3.08**	0.65	148	−6
JAR	5.8	−0.30	2.23	0.77	120	−9
Dye-2	7.3	−0.46	2.72	0.73	159	−6
Average		0.59	2.47	0.76		−6

variables are shown in Figs. 3–6. The model output used to calculate the verification statistics and to plot the monthly time series is available at 3-h intervals, unless otherwise noted, while the AWS observations are available at 1-h intervals.

The six GC-NET AWS sites used for model verification purposes are shown in Fig. 1b (Humboldt: HU; Tunu-N: TU; Summit: SU; Crawford Point: CP; JAR 1: JA; Dye-2: D2) and were selected to represent as wide an area of the Greenland ice sheet as possible, while confining the choice of stations to those with nearly complete records for April and May 1997. Results from these six stations are comparable to those from the other GC-NET AWS sites on Greenland. Only site A4 from the KABEG'97 AWS array is used for model verification (Figs. 1b,c), as the remaining KABEG'97 AWS sites are located close to the ice margin and over the adjacent tundra in a region of small-scale terrain features that are poorly represented by the 40-km model grid used in this study.

Before presenting results of the model–AWS comparison it should be noted that the AWS measured temperature and wind speed are from heights of generally less than 3 m AGL. In contrast, the modeled temperature and wind speed from the Polar MM5 are taken from the lowest σ level, with a nominal height of 12 m AGL. The wind speed from the lowest model level has been interpolated to the height of the AWS observations by applying Monin–Obukhov similarity theory. No attempt to adjust the modeled temperature to an equivalent height above the snow surface has been made. Differences in the modeled and observed air temperature, due to differences in the observation and simulation heights, will be largest during periods of light winds but should be minimal otherwise. The modeled pressure has been adjusted to the reported elevation of the AWS sites using the model gridpoint elevation and the observed air temperature at the AWS sites.

TABLE 5. (*Continued*)

Station	Wind speed: Mean (m s^{-1})	Bias (m s^{-1})	Rmse (m s^{-1})	Corr	Resultant wind direction: Mean (deg)	Bias (deg)
Humboldt	5.6	0.98	1.93	0.60	184	−10
Tunu	5.4	−0.04	1.40	0.67	277	0
Summit	3.6	**1.05**	2.17	0.43	205	**−18**
Crawford	6.1	0.92	2.53	0.57	148	−8
JAR	6.2	−0.53	2.69	**0.68**	125	11
Dye-2	7.0	−0.54	**2.75**	0.54	162	−9
Average		0.31	2.25	0.58		−6

Based on an inspection of Figs. 3–6 it appears that the Polar MM5 reproduces the observed time series of surface pressure, temperature, wind speed, wind direction, and mixing ratio with a surprising degree of accuracy during the two-month period of April–May 1997. A noticeable bias in the surface pressure is evident at some of the sites and is due, in part, to uncertainties of ± 20 m in the true elevation of the AWS sites. A warm bias in the model forecast near-surface temperature is present at the Summit (Fig. 4) and A4 (Fig. 6) AWS sites. Daily spikes, of up to 3 hPa, in the observed pressure at Tunu AWS are measurement errors (Fig. 3).

A review of Tables 4–6 reveals the generally high level of skill exhibited by the Polar MM5 forecasts. The magnitude of the surface pressure bias ranges from 0.09 to 6.63 hPa, with the magnitude of the bias generally less than 3 hPa at most sites. Part of the bias in the surface pressure can be attributed to the uncertainty in the true elevation of the AWS sites. [The elevation of AWS sites Summit, Crawford Point, Dye-2, and A4 were determined with a handheld GPS receiver and are known to within ± 20 m, while the elevation at the remaining AWS sites was determined using differential GPS measurements (Table 2) and are known to an accuracy of ± 0.1 m.] An uncertainty in the elevation of the AWS site of ± 20 m implies an uncertainty in the adjusted model pressure of ± 2 hPa. This level of uncertainty in the adjusted model pressure can account for some, but not all, of the bias in the comparison of the modeled and observed surface pressures. The modeled monthly mean surface pressure does not increase as much as the observed surface pressure from April to May, for all of the GC-NET AWS sites, resulting in the model bias in the surface pressure becoming increasingly negative with time (Tables 4 and 5). The source of the differences in surface pressure between the Polar MM5 forecasts and the AWS observations are still being explored. The large bias in the pressure at Tunu-N is likely caused in part by a measurement error at this site (note the anomalous spikes in the observed pressure that occur on a daily basis in Fig. 3).

The rmse of the surface pressure ranges from 1.43 to 6.91 hPa and is an indication of the typical instantaneous magnitude of the difference between the modeled and observed surface pressure. The correlation coefficient between the modeled and observed surface pressure is high, ranging from 0.93 to 0.99, indicating that the Polar

TABLE 6. Same as Table 4, except for KABEG AWS A4 for 16 Apr–17 May 1997.

	Surface pressure				Temperature				Wind speed				Resultant wind direction	
Station	Mean (hPa)	Bias (hPa)	Rmse (hPa)	Corr	Mean (K)	Bias (K)	Rmse (K)	Corr	Mean (m s^{-1})	Bias (m s^{-1})	Rmse (m s^{-1})	Corr	Mean (deg)	Bias (deg)
A4	837	−3.80	4.20	0.99	−16.5	3.81	5.01	0.90	5.6	1.36	2.63	0.68	146	0

MM5 forecasts reproduce the observed trends in the surface pressure accurately (as is evident from Figs. 3–6). The lower correlation coefficient values between the model and observed pressure at Tunu-N AWS are caused in part by the anomalous daily spikes in the observed pressure at this site (Fig. 3).

The monthly bias in temperature has a magnitude of less than ≈1 K at most sites, but is significantly larger than 1 K at both Summit and A4 (Tables 3–5). The average bias in the Polar MM5 simulations at the GC-NET AWS sites increases from 0.35 to 1.07 K from April to May (Tables 3 and 4). Preliminary investigation of the radiative fluxes at the surface in the Polar MM5 simulations indicates an excess of downward-directed shortwave radiation, which may contribute to the increasing warm bias as the summer solstice is approached.

The rmse ranges from 2.5 to 5 K at most sites, with correlation coefficients between the observed and modeled near-surface temperature greater than 0.83 for all sites for both months.

The forecast near-surface temperature from the Polar MM5 reproduces the observed diurnal temperature range at most sites (Figs. 3–6). A notable exception is at Summit AWS (Fig. 4), where the Polar MM5 forecast of the daily minimum temperature is often too warm (Julian days 111–116, 121–124, 128–132, and 135–147). This error in the modeled minimum temperature at Summit is responsible for the large temperature bias at this site (Tables 3 and 4). The time periods with overly warm minimum temperature in the Polar MM5 forecasts also correspond to time periods with weak wind speeds (<5 m s^{-1} in both the observations and model forecasts), when a strong low-level inversion would be expected to be present. A portion of the warm bias at Summit may be attributed to the difference in the height above the snow surface of the modeled and observed air temperature, in the presence of a strong low-level inversion. To evaluate this possibility the time series of the model predicted ground temperature is compared to the observed near-surface air temperature measured at the AWS. From this comparison (not shown) it is found that on most of the days when the Polar MM5 simulates overly warm minimum near-surface air temperatures the forecast ground temperature was equal to, or slightly colder, than the AWS observed near-surface air temperature. Therefore a portion of the warm bias in the Polar MM5 forecasts is a result of the strong inversion conditions present near the surface during the light wind periods and the different height of the AWS observation and the model's lowest atmospheric level. Additionally, the strong low-level inversion and weak winds combine to generate enhanced static stability near the surface. It is well known that atmospheric surface-layer parameterizations do not adequately represent the turbulent coupling of the atmosphere to the surface under these strong static stability conditions (Cassano et al. 2001) and can lead to overly warm near-surface atmospheric temperatures being predicted in the model.

In addition to accurately simulating the diurnal tem-

TABLE 7. Statistics from the comparison of the Polar MM5 simulated vertical profiles to the KABEG aircraft profile data for Apr and May 1997, for potential temperature and wind speed. Statistics listed in the table include the vertically averaged difference between the Polar MM5 and aircraft data (bias) (Polar MM5 − aircraft), the root-mean-square error (rmse), and the correlation coefficient between the Polar MM5 and aircraft data (corr). For each aircraft profile the flight number is listed followed by the number of hours elapsed since the start of the Polar MM5 forecasts (forecast time). Maximum absolute values are printed in bold and minimum absolute values are underlined for the bias, rmse, and correlation coefficient for each variable.

	Potential temperature			Wind speed		
Flight number; forecast time (h)	Bias (K)	Rmse (K)	Corr	Bias (m s^{-1})	Rmse (m s^{-1})	Corr
KA1; +30/+33	2.3/0.9	2.4/1.2	0.99/0.99	−7.5/−7.1	7.5/7.2	0.97/0.90
KA2; +30/+33	1.4/1.3	2.5/2.4	0.81/8.85	−4.8/−1.1	5.9/2.3	−0.08/0.77
KA3; +30/+33	−2.4/−1.7	2.6/1.9	**1.00**/**1.00**	5.3/4.5	5.6/4.7	0.84/0.88
KA4; +33/+36	2.4/3.1	2.5/3.1	0.93/0.98	−3.4/−4.6	3.5/4.6	0.93/0.96
KA5; +30/+33	2.9/**3.6**	3.3/**3.9**	0.91/0.92	0.6/0.6	1.8/1.9	0.94/0.97
KA6; +30/+33	2.0/1.8	2.1/1.8	0.99/0.99	−1.4/−2.3	1.5/2.4	**0.99**/0.98
KA8; +30/+33	0.2/0.4	1.4/1.0	0.96/0.99	2.7/−0.4	2.7/1.0	**0.99**/0.97
KA9; +30/+33	−0.1/0.0	2.1/2.3	0.97/0.96	11.6/**12.5**	12.0/**12.8**	0.84/0.87
Average	1.1/1.2	2.4/2.2	0.95/0.96	0.4/0.3	5.1/4.6	0.80/0.91

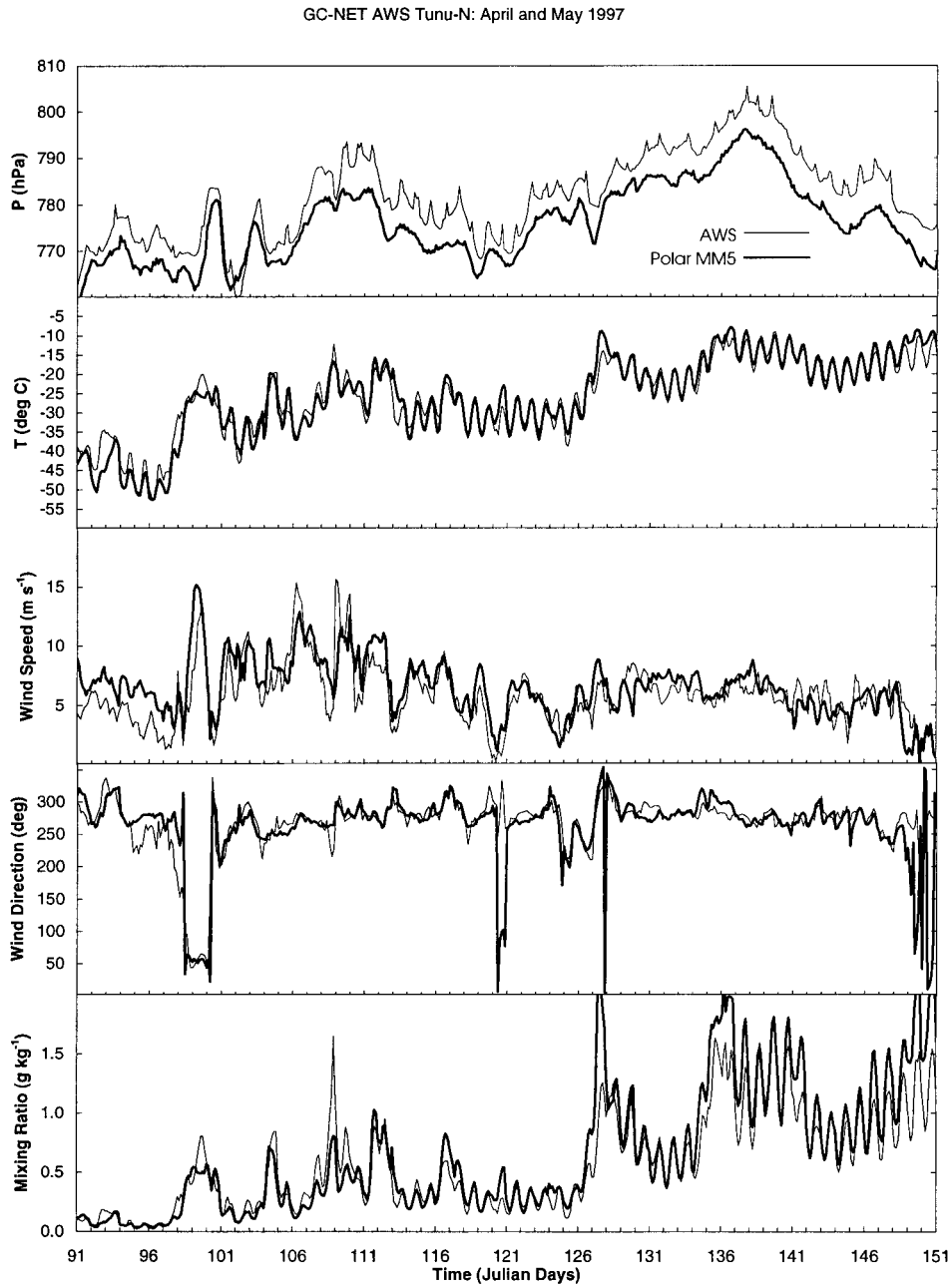

FIG. 3. Time series of the 24–48-h Polar MM5 forecasts (thick, solid line) and the Tunu-N AWS observations (thin, solid line) for Apr and May 1997. Time series of surface pressure (P), near-surface air temperature (T), wind speed, wind direction, and water vapor mixing ratio are plotted. The time axis is labeled in Julian days (1 Apr 1997 = Julian day 91 and 1 May 1997 = Julian day 121). The surface pressure for the Polar MM5 forecast has been interpolated from the height of the model gridpoint elevation to the height of the AWS observations. The model wind speed has been interpolated from the lowest model level to the height of the AWS observations. All other Polar MM5 variables are given as the value at the lowest model sigma level (nominal height of 12 m AGL), and are not corrected for differences between the elevation of the model grid point and the reported elevation of the AWS.

perature cycle, the Polar MM5 forecast temperatures also replicated the large-scale changes in temperature quite well. As an example, the abrupt warming observed at Tunu-N on Julian day 97 and at Dye-2 and Summit on Julian day 100 are all simulated accurately by the Polar MM5.

Comparison of the modeled and observed near surface mixing ratio of water vapor indicates a slight moist

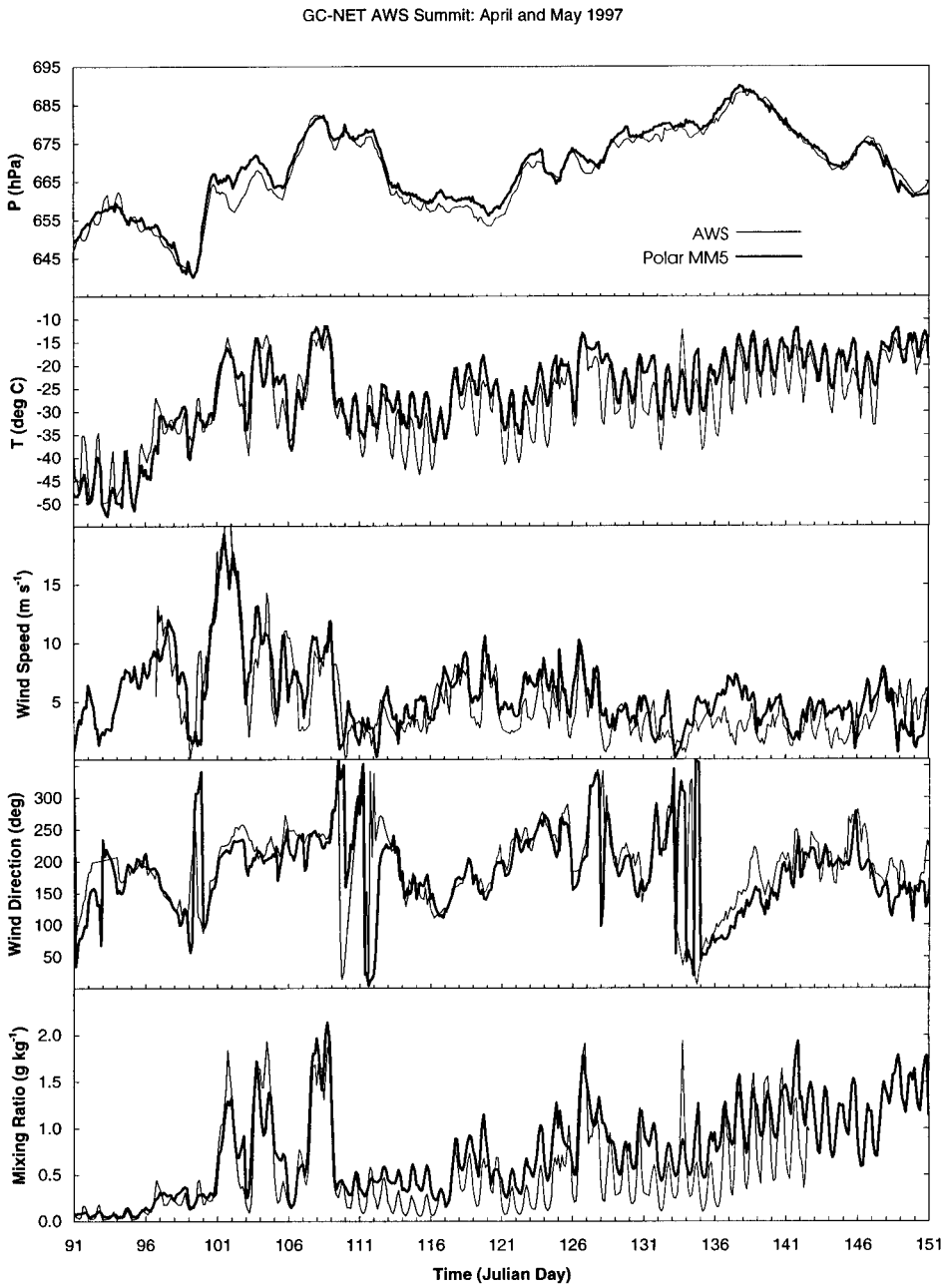

FIG. 4. Same as Fig. 3, except for Summit AWS.

bias in the Polar MM5 forecasts (Tables 3 and 4, Figs. 3–6). The absolute magnitude of the bias increases from April to May, due in part to the increasing amount of moisture present in the atmosphere, although the magnitude of the bias relative to the mean mixing ratio also increases from April to May. The largest relative errors occur at the northern AWS sites of Humboldt and Tunu-N and at Summit. The increase in the low-level moist bias in the Polar MM5 forecasts during May coincides with an increasing warm bias in the Polar MM5 forecast for the same time period. This highlights the importance of accurate near-surface temperature forecasts for skillful forecasts of the low-level moisture content of the air.

Aside from the slight moist bias in the Polar MM5 forecasts, the time series of the modeled mixing ratio is similar to the observed time series. Correlation coefficients between the two time series range from 0.77 to 0.93. The rmse ranges from 0.11 to 0.49 g kg^{-1}, with larger values found for May compared to April.

Finally, the modeled near-surface winds are in good agreement with the observed winds at most of the sites,

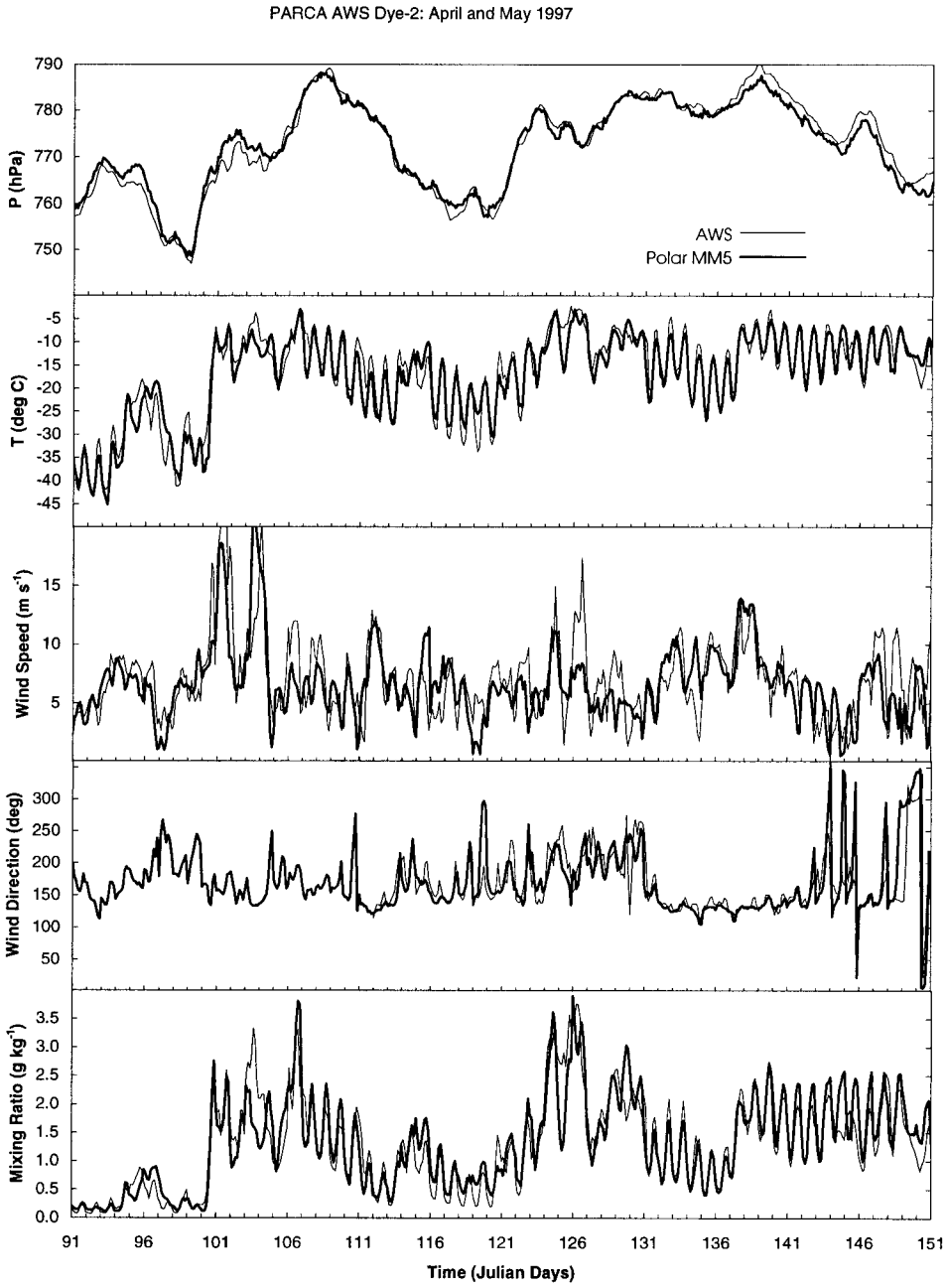

FIG. 5. Same as Fig. 3, except for Dye-2 AWS.

although the modeled wind speed tends to be slightly less variable than the observed wind speed on time periods shorter than 24 h (Figs. 3–6). The magnitude of the bias in the wind speed forecasts ranges from −0.03 to 1.59 m s^{-1}, with magnitudes of the bias generally less than 1 m s^{-1}. The rmse varies from 1.40 to 3.08 m s^{-1}, and the correlation coefficient between the observed and model wind speed time series ranges from 0.43 to 0.84. The lower correlation coefficient for the wind speed forecasts, compared to the other variables discussed above, is a result of the smaller variability in the modeled wind speeds compared to the observations.

The magnitude of the bias in the resultant wind direction is generally less than 10°, with the largest bias at Summit (18° for May 1997). As with the other variables, the Polar MM5 predicted wind direction matches the observed changes in the wind direction quite accurately (Figs. 3–6). Of particular note is the excellent agreement between the observed and modeled wind direction change at Tunu-N on Julian days 98 to 101 (Fig.

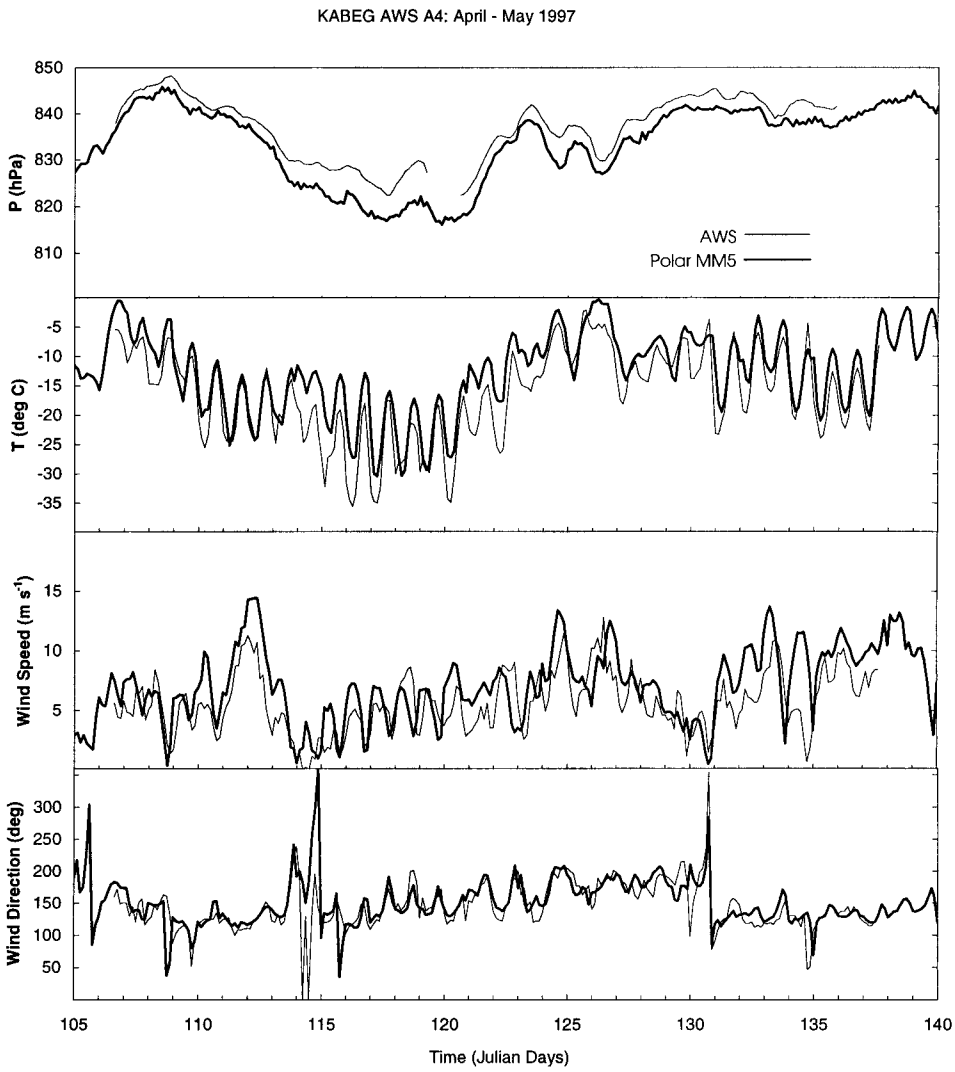

FIG. 6. Same as Fig. 3, except for KABEG AWS A4. Data is plotted from 15 Apr to 20 May 1997 (Julian days 105–140).

3) and the suppressed variability in the modeled and observed wind direction at Dye-2 on Julian days 131–143 (Fig. 5).

In summary, the Polar MM5 forecasts of the pressure, temperature, mixing ratio, and winds compare very favorably with the AWS observations. The Polar MM5 near-surface temperature is particularly well forecast, with slightly reduced skill for the near-surface wind forecasts.

c. Verification of the Polar MM5 forecasts with aircraft observations

Aircraft data collected during the KABEG'97 field program provided an opportunity to verify the katabatic layer structure simulated by the Polar MM5. As discussed in section 2, vertical profiles through the katabatic layer were measured by the aircraft during a series of ascents and descents. Each ascent–descent through the katabatic layer (over a depth of approximately 400 m) covered a horizontal distance of roughly 5 km, and as such does not represent a true vertical profile. For each flight period (Table 1) the aircraft profile over the location farthest from the ice sheet margin (Fig. 1b) was compared to the modeled vertical profiles of the katabatic layer, using the grid point closest to the location of the aircraft profile. These aircraft profiles were chosen for comparison to the model data, since the model horizontal resolution is not suited for representation of the steep ice slopes closest to the ice sheet margin.

Flights KA1 through KA5 and flight KA8 took place near location A4, shown in Figs. 1b and 1c, in a region of relatively uniform ice topography. The aircraft profiles for flights KA6 and KA9 were measured near points

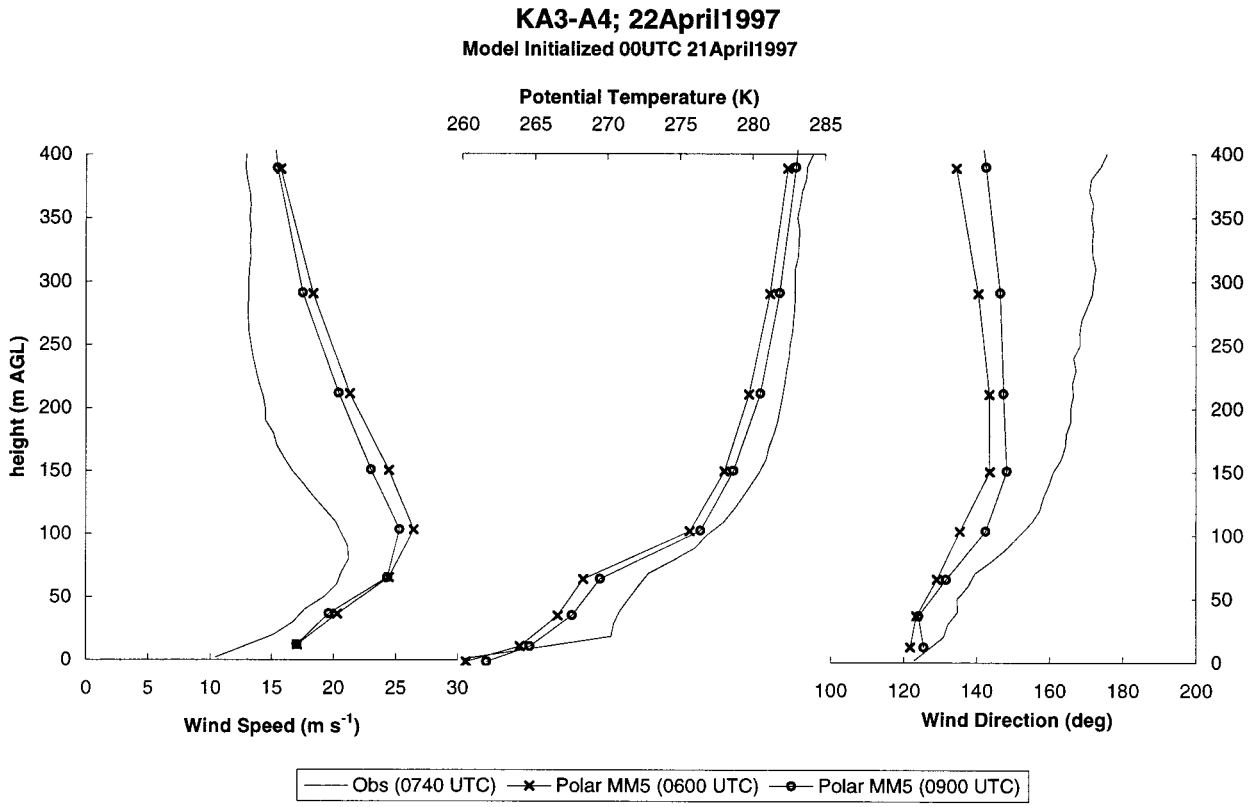

FIG. 7. Vertical profiles of wind speed, potential temperature, and wind direction from the 30-h (valid at 0600 UTC 22 Apr 1997, plotted as a thin, solid line with cross symbols) and 33-h (valid at 0900 UTC 22 Apr 1997, plotted as a thin, solid line with open circle symbols) Polar MM5 forecasts initialized at 0000 UTC 21 Apr 1997 and aircraft observations (plotted as a thin, solid line) from 0740 UTC 22 Apr 1997 for KABEG flight KA3 at location A4. Profiles are plotted with respect to height above the ground (m AGL) to a height of 400 m AGL.

P4 and I4, respectively, in Fig. 1b, and are located in regions with pronounced valley-like features in the ice sheet topography, that act to channel the katabatic flow.

Comparison of the observed and modeled potential temperature, wind speed, and wind direction profiles are presented below. Summary statistics from the comparison of the modeled vertical profiles to the observed aircraft profiles for the eight flights are listed in Table 7. Statistics are calculated for the two model times that bracketed the time of the aircraft observation (this corresponds to forecasts valid 30–36 h after the Polar MM5 was initialized). Average statistics for all eight flight periods are also listed at the bottom of Table 7.

As was found for the verification of the near surface variables with the AWS data, on average the Polar MM5 forecast potential temperature profiles are in better agreement with the observations than the forecast wind profiles. This is evident as larger correlation coefficients for the potential temperature forecasts as well as smaller rmse (Table 7).

The average correlation coefficient for all eight flights for the potential temperature profiles is 0.95 to 0.96 for both model time periods considered. The average bias of the predicted potential temperature profiles varies from 1.1 to 1.2 K, while the rmse ranges from 2.2 to 2.4 K (Table 7). These values are similar to those found for the near-surface temperature verification (Tables 4–6).

The predicted wind speed profiles do not match the observed wind speed profiles as well as the potential temperature profiles. Average correlation coefficients for the wind speed profiles range from 0.80 to 0.91, which is slightly larger than the results for the near-surface verification. The magnitude of the average bias in the predicted wind speed profiles is 0.3 to 0.4 m s^{-1} for both forecast periods, but these surprisingly low values are the result of large biases of opposite signs for individual flights (i.e., KA1 and KA9) that nearly cancel. The rmse of the modeled wind speed profiles range from 4.6 to 5.1 m s^{-1} and is larger than the average rmse for the modeled near-surface wind speeds (Tables 4–6).

Based on the average verification statistics for the eight KABEG'97 aircraft profiles it appears that the Polar MM5 forecasts through the depth of the katabatic layer are generally as skillful as the near-surface forecasts discussed in section 4b. We will now examine three of the aircraft flights in more detail.

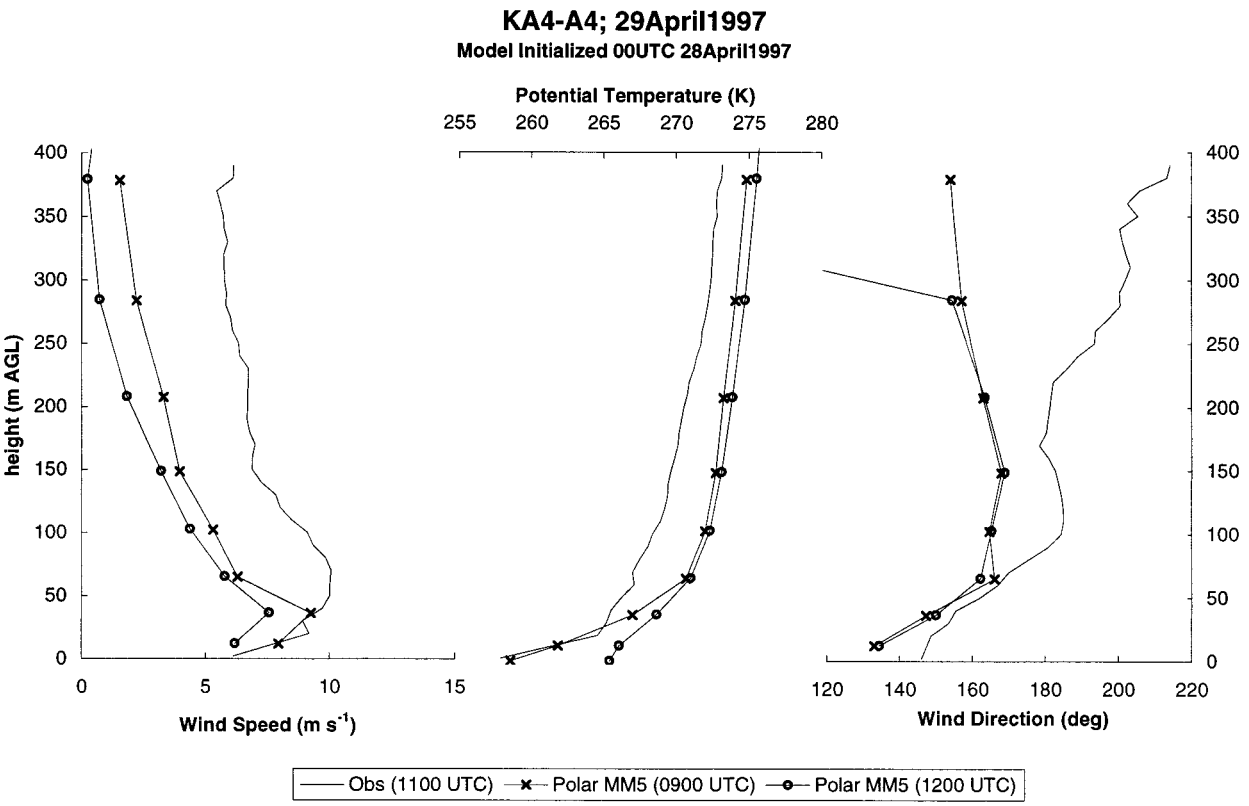

FIG. 8. Same as Fig. 7, except model profiles are 33 h (valid at 0900 UTC 29 Apr 1997) and 36 h (valid at 1200 UTC 29 Apr 1997) Polar MM5 forecasts initialized at 0000 UTC 28 Apr 1997, and aircraft observations are from 1100 UTC 29 Apr 1997 for KABEG flight KA4 at location A4.

1) FLIGHT KA3

Flight KA3 was selected for detailed analysis since it represents a case with moderate large-scale forcing for the katabatic wind. In addition, no cloud cover was observed over the ice sheet during the flight, and strong surface winds caused drifting snow near the surface.

Figure 7 displays the modeled and observed profiles of potential temperature, wind speed, and wind direction for flight KA3. From the figure it is evident that the Polar MM5 simulates a slightly stronger katabatic jet, located approximately 30 m higher than was observed. The bias for the modeled wind speed profile for these time periods is 4.5–5.3 m s^{-1}, with a correlation coefficient of 0.84–0.88. The modeled potential temperature profile is similar to the observed profile (correlation coefficient of 1.00 for both forecast periods), although the model simulates an overly strong elevated inversion between 50 and 100 m AGL, and a weaker surface based inversion than is observed, and has a slight bias of -2.4 to -1.7 K. Finally, the wind direction profiles are of similar shape, with both the modeled and observed winds veering with increasing height, toward a more cross-slope direction, although the modeled winds are offset from the observations by up to 40°, particularly near the top of the aircraft profiles (400 m AGL).

Taking the wind observations at 400 m AGL to represent the large-scale forcing for the katabatic wind it is found that the Polar MM5 forecast has overly strong winds at this level (approximately 3 m s^{-1} larger) and wind directions that are directed in a more downslope direction by 40°. These errors in the large-scale forcing likely explain the differences between the modeled and observed profiles in the katabatic layer. The source of this error in the large-scale forcing is unclear and may represent an error in the model initial and boundary conditions derived from the ECMWF analyses or may represent an error in the evolution of the atmospheric mass fields during the 30–36-h simulation.

2) FLIGHT KA4

Flight KA4 represents a complex situation that had relatively weak large-scale pressure gradients present in the region of the aircraft flight. In addition, this flight was made during the late morning, 1100 UTC, when the katabatic wind was decaying. Also, clouds during the overnight period before the flight limited the amount

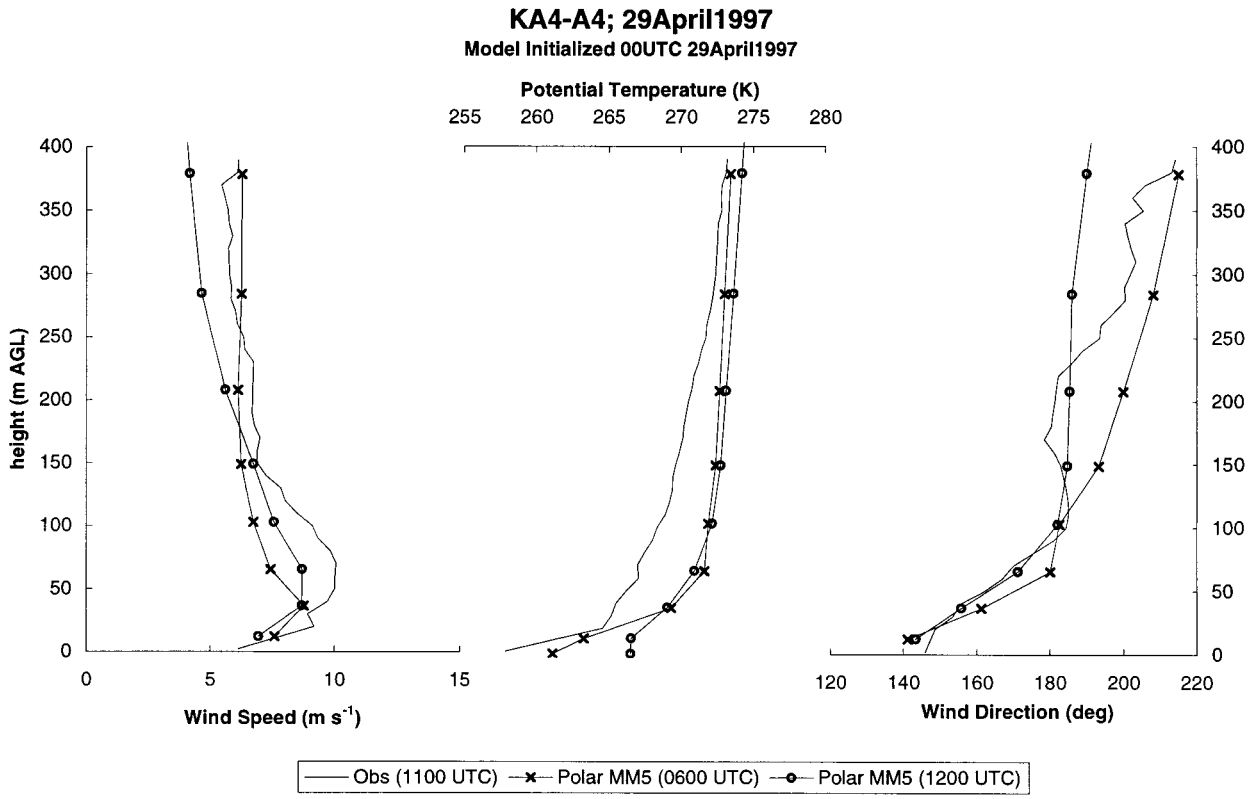

FIG. 9. Same as Fig. 8, except model profiles are 6 h (valid at 0600 UTC 29 Apr 1997) and 12 h (valid at 1200 UTC 29 Apr 1997) Polar MM5 forecasts initialized at 0000 UTC 29 Apr 1997.

of surface cooling thus inhibiting strong katabatic wind development.

Observed and modeled profiles of wind speed, potential temperature, and wind direction for flight KA4 are shown in Fig. 8. The Polar MM5 underestimates the wind speed from the surface to 400 m AGL (bias of -4.6 to -3.4 m s^{-1}) and the potential temperature is overestimated over much of this depth (bias of 2.4–3.1 K). As with the model comparison to the aircraft data for flight KA3, the simulated flow at 400 m AGL differs from that observed by the aircraft, indicating that the large-scale forcing for the katabatic circulation is incorrect in the model, either due to an error in the ECMWF analyses or to an incorrect readjustment of the atmospheric mass in the model domain during the simulation. For flight KA4 this error in the large-scale forcing leads to weaker winds in the model relative to the aircraft observations.

Model profiles valid at 0600 and 1200 UTC, from a simulation initialized at 0000 UTC 29 April (6- and 12-h forecasts), are compared to the observed profiles in Fig. 9. For these shorter forecasts, initialized 24 h after the forecasts shown in Fig. 8, there is much better agreement in the wind speed and wind direction between the model and the observations from the surface to 400 m AGL. This better agreement may result from more accurate model initial conditions for the later forecast period or may reflect the shorter time for model errors to become evident in the simulation. Without further observations of the upper-level winds it is not possible to unambiguously determine the source of the error in the simulated katabatic layer profiles.

The importance of an accurate representation of cloud cover and the radiative properties of clouds is explored with an additional Polar MM5 simulation for flight KA4. The sensitivity simulation uses the Polar MM5 but does not include the modified representation of cloud radiative properties described in section 3a (the cloud radiative properties in the sensitivity simulation are based solely on the gridpoint relative humidity and temperature). Results from this unmodified radiation parameterization simulation are shown in Figs. 10 and 11.

In Fig. 10 the evolution of the near-surface air temperature, wind speed, wind direction, and cloud cover in the standard Polar MM5 simulation (heavy line) is compared to that in the unmodified radiation parameterization simulation (heavy dashed line). Both simulations overestimate the near-surface air temperature during the 48-h simulation when compared to the AWS observations. This error is due, in part, to an error in the model initial conditions, which are 15°C warmer than is observed at the AWS. (It should be noted that

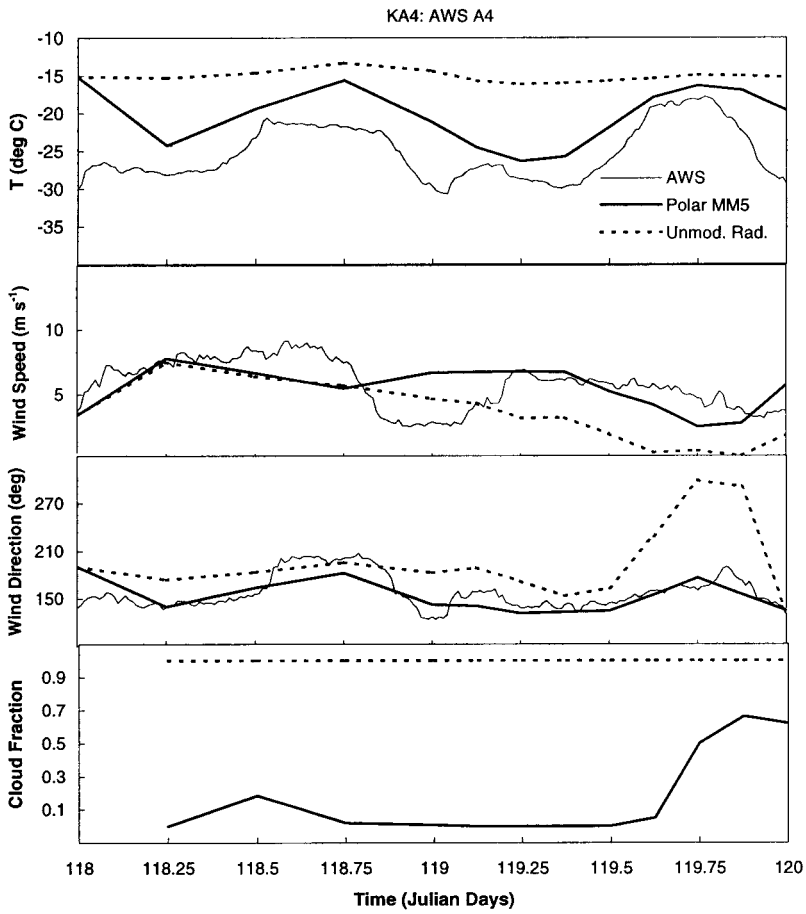

FIG. 10. Two-day time series plots of temperature (T), wind speed, wind direction, and cloud fraction from the Polar MM5 forecasts (thick, solid line) initialized at 0000 UTC 28 Apr 1997 and observations from KABEG AWS A4 (thin, solid line; no observations of cloud fraction). Model output from a Polar MM5 simulation without the modified radiation parameterization is plotted as a thick, dashed line in each panel. The time axis is labeled in Julian days (28 Apr 1997 = Julian day 118). Data from the Polar MM5 forecasts are plotted every 6 h on Julian day 118, and every 3 h on Julian day 119.

errors in the model initial temperature were common throughout the two months of simulations.) The Polar MM5 simulated air temperature rapidly cools from the incorrect initial temperature and accurately represents the diurnal temperature changes during the 48-h simulation. In contrast, the Polar MM5 simulation without the modified radiation parameterization experiences little cooling and little diurnal temperature change. This is caused by overcast conditions, and radiatively thick clouds, being simulated by the unmodified radiation parameterization. The error in the cloud radiative properties reduces both heating from shortwave radiation and cooling due to longwave radiative losses from the surface. The error in the near-surface air temperature also leads to an unrealistic decay in the katabatic flow over the 48-h simulation.

The simulated vertical structure of the katabatic layer from the sensitivity simulation is shown in Fig. 11. No low-level temperature inversion is simulated (consistent with the overcast conditions and warm surface temperature simulated) and no katabatic jet is present in the simulation. The results from this sensitivity simulation illustrate the importance of accurate representation of cloud–radiation interaction for the simulation of katabatic winds.

3) FLIGHT KA8

The synoptic situation for flight KA8 was dominated by a surface high pressure located over central Greenland. This feature generated a strong pressure gradient that acted to support katabatic wind development in the area of the research flight. Some high clouds were also observed during the flight, the timing of which are simulated correctly by the Polar MM5 (not shown).

The 30- and 33-h Polar MM5 forecast profiles (valid

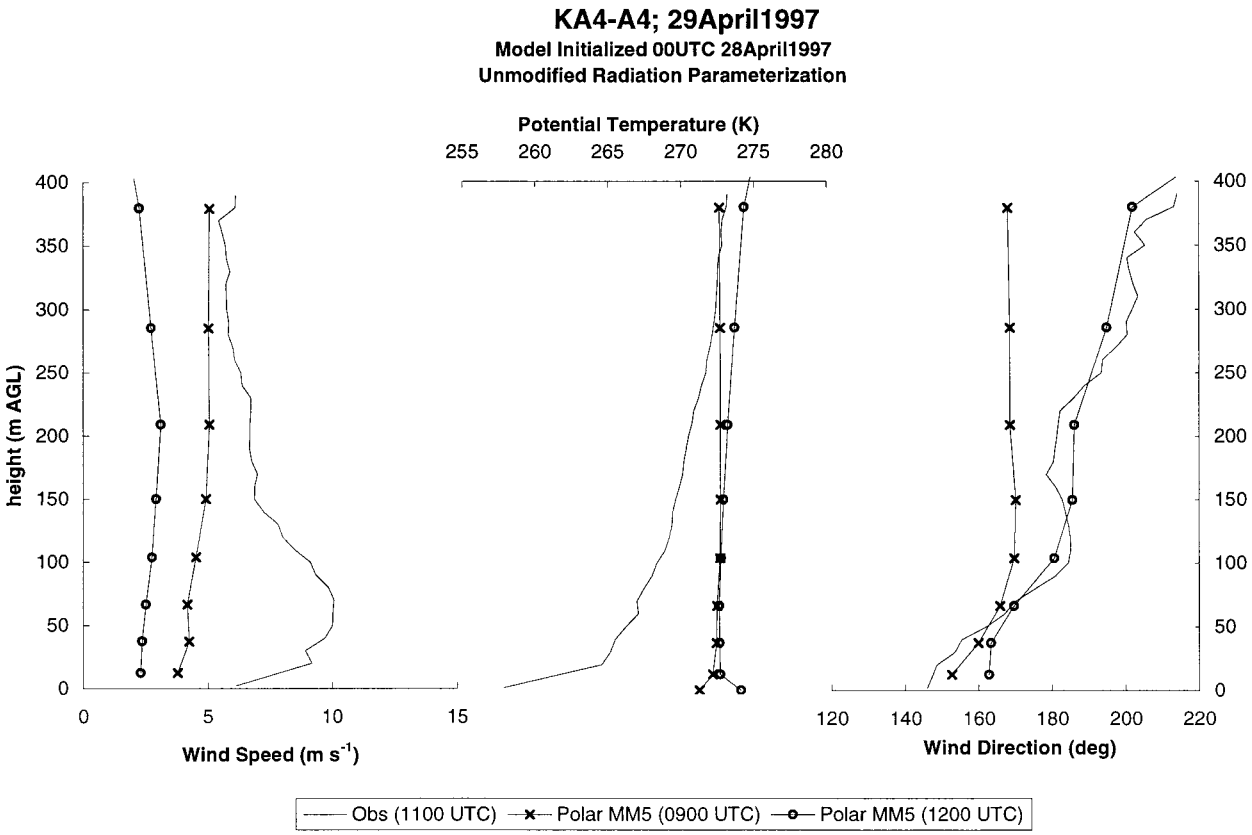

FIG. 11. Same as Fig. 8, except output from a Polar MM5 simulation with the unmodified radiation parameterization is plotted.

at 0600 and 0900 UTC 13 May) are compared to the observed profiles in Fig. 12. For this case the Polar MM5 produced an excellent simulation of the katabatic layer winds and temperature (Table 7). The modeled and observed potential temperature profiles agree in both magnitude and shape through the lowest 400 m of the atmosphere, with a slight warm bias in the modeled near-surface temperature (bias of 0.2–0.4 K, correlation coefficient of 0.96–0.99). Similarly, there is good agreement between the modeled and observed wind speed profiles (bias of -0.4 to 2.7 m s^{-1}, correlation coefficient of 0.97–0.99) and wind direction profiles.

5. Conclusions

A comparison of two months of simulations from the Polar MM5 model with ECMWF operational analyses, AWS observations, and aircraft observations from the Greenland ice sheet have been presented. The verification indicates that the Polar MM5 simulates both the large-scale and low-level atmospheric features over the Greenland ice sheet with a high degree of realism.

Near-surface temperature and wind speed forecasts had mean errors (biases) of less than 1 K and 1 m s^{-1} for most of the AWS sites considered. Larger errors in the near-surface air temperature are evident for cases with weak winds and strong static stability, and reflect the difficulty of accurately parameterizing the surface-layer turbulent fluxes under these conditions. The source of errors in the mean surface pressure between the model and observations could not be determined unambiguously, although a portion of the pressure errors (at some AWS sites) is likely caused by uncertainty in the elevation of the AWS sites. The Polar MM5 has a slight moist bias near the surface, as revealed by the comparison of the predicted and observed near-surface water vapor mixing ratio.

The wind and potential temperature profiles within the katabatic layer over the Greenland ice sheet are also simulated with a high degree of skill, based on comparisons with aircraft observations. Sensitivity simulations indicate that the model skill is sensitive to errors in the large-scale forcing and the representation of key physical processes.

The simulated katabatic flow is sensitive to errors in the large-scale pressure gradient. Large biases (magnitude > 5 m s^{-1}) in the wind speed profiles are found for certain aircraft flights (e.g., KA1 and KA9). The errors in the large-scale pressure gradient, inferred from differences in the modeled and aircraft observed wind speeds at 400 m AGL, for these simulations may be caused by errors in the atmospheric analyses used for initial and boundary conditions in the models, by errors in the propagation speed of atmospheric features

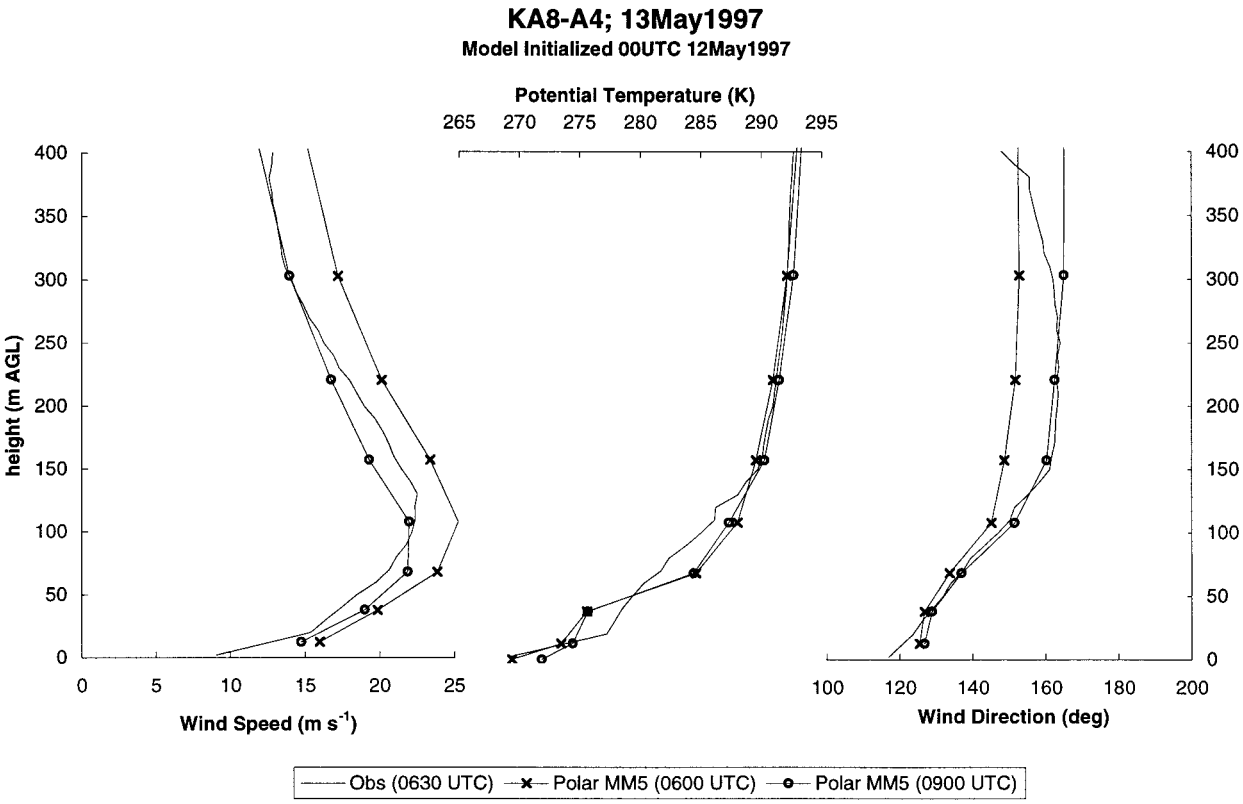

FIG. 12. Same as Fig. 7, except model profiles are 30 h (valid at 0600 UTC 13 May 1997) and 33 h (valid at 0900 UTC 13 May 1997) Polar MM5 forecasts initialized at 0000 UTC 12 May 1997, and aircraft observations are from 0630 UTC 13 May 1997 for KABEG flight KA8 at location A4.

through the model domain, or by errors in the redistribution of atmospheric mass within the model domain. For all of the simulations with large wind speed biases, additional simulations initialized closer to the time of the aircraft flights have reduced wind speed biases and smaller differences between the observed and modeled wind speeds at 400 m AGL.

The modeled katabatic layer is also found to be sensitive to errors in the predicted cloud cover, and to the radiative properties of the clouds. For flight KA4, a Polar MM5 sensitivity experiment that did not use the modified radiation parameterization predicts thick cloud cover during the 48-h simulation leading to minimal cooling of the near-surface air and an erroneous simulation of the katabatic flow. The fully modified Polar MM5 simulation does not simulate a thick cloud cover during the 48-h model run and thus has a more accurate representation of the temperature and wind profiles in the katabatic layer. These results indicate the utility of using the model-predicted cloud water and ice mixing ratios to determine the radiative properties of the clouds, and they highlight the tremendous sensitivity that cloud and radiation parameterizations can have on simulated katabatic flows.

Simulations for an entire annual cycle, over Greenland, are currently under way using the Polar MM5. In addition, further research and validation of the radiative forcing in Polar MM5 is continuing, using the radiation observations from the GC-NET AWS array.

Acknowledgments. This research was funded by National Science Foundation Grants OPP-9707557 and OPP-9905381 to DHB. The international collaboration between DHB, JJC, KMH, TK and GH was supported in part by National Science Foundation Grant INT-9603416 to DHB and KMH. Funding for the GC-NET AWS array was provided by NSF Grant OPP-9423530 and NASA Grant NAGS-4248 to KS. The global ECMWF analyses used in this project were provided by ECMWF and were distributed by the Data Support Section of the Scientific Computing Division of NCAR. Use of the computer resources at NCAR was funded through Grant 3706880. Comments from three anonymous reviewers helped to improve this manuscript.

REFERENCES

Bromwich, D. H., Y. Du, and T. R. Parish, 1994: Numerical simulation of winter katabatic winds from West Antarctica crossing Siple Coast and the Ross Ice Shelf. *Mon. Wea. Rev.*, **122,** 1417–1435.

——, ——, and K. M. Hines, 1996: Wintertime surface winds over the Greenland ice sheet. *Mon. Wea. Rev.*, **124,** 1941–1947.

Cassano, J. J., and T. R. Parish, 2000: An analysis of the nonhy-

drostatic dynamics in numerically simulated Antarctic katabatic flows. *J. Atmos. Sci.,* **57,** 891–898.
——, ——, and J. C. King, 2001: Evaluation of turbulent surface flux parameterizations for the stable surface layer over Halley, Antarctica. *Mon. Wea. Rev.,* **129,** 26–46.
Curry, J. A., and Coauthors, 2000: FIRE Arctic Clouds Experiment. *Bull. Amer. Meteor. Soc.,* **81,** 5–29.
Dudhia, J., 1993: A nonhydrostatic version of the Penn State–NCAR mesoscale model: Validation tests and simulation of an Atlantic cyclone and cold front. *Mon. Wea. Rev.,* **121,** 1493–1513.
Ebert, E. E., and J. A. Curry, 1992: A parameterization of ice cloud optical properties for climate models. *J. Geophys. Res.,* **97,** 3831–3836.
Ekholm, S., 1996: A full coverage, high-resolution, topographic model of Greenland computed from a variety of digital elevation data. *J. Geophys. Res.,* **101,** 21 961–21 972.
Fletcher, N. H., 1962: *Physics of Rain Clouds.* Cambridge University Press, 386 pp.
Gallée, H., and G. Schayes, 1992: Dynamical aspects of katabatic wind evolution in the Antarctic coastal zone. *Bound.-Layer Meteor.,* **59,** 141–161.
——, and P. G. Duynkerke, 1997: Air–snow interaction and the surface energy mass balance over the melting zone of west Greenland during the Greenland Ice Margin Experiment. *J. Geophys. Res.,* **102,** 13 813–13 824.
Gloersen, P., W. J. Campbell, D. J. Cavalieri, J. C. Comiso, C. L. Parkinson, and H. J. Zwally, 1992: *Arctic and Antarctic Sea Ice, 1978–1987: Satellite Passive–Microwave Observations and Analysis.* National Aeronautics and Space Administration, 290 pp.
Grell, G. A., J. Dudhia, and D. R. Stauffer, 1994: A description of the fifth-generation Penn State/NCAR mesoscale model (MM5). NCAR Tech. Note NCAR/TN-398+STR, 122 pp.
Hack, J. J., B. A. Boville, B. P. Briegleb, J. T. Kiehl, P. J. Rasch, and D. L. Williamson, 1993: Description of the NCAR community climate model (CCM2). NCAR Tech. Note NCAR/TN-382+STR, 108 pp.
Heinemann, G., 1997: Idealized simulations of the Antarctic katabatic wind system with a three-dimensional mesoscale model. *J. Geophys. Res.,* **102,** 13 825–13 834.
——, 1999: The KABEG'97 field experiment: An aircraft-based study of katabatic wind dynamics over the Greenland ice sheet. *Bound.-Layer Meteor.,* **93,** 75–116.
Hines, K. M., D. H. Bromwich, and T. R. Parish, 1995: A mesoscale modeling study of the atmospheric circulation of high southern latitudes. *Mon. Wea. Rev.,* **123,** 1146–1165.
——, ——, and Z. Liu, 1997a: Combined global climate model and mesoscale model simulations of Antarctic climate. *J. Geophys. Res.,* **102,** 13 747–13 760.
——, ——, and R. I. Cullather, 1997b: Evaluating moist physics for Antarctic mesoscale simulations. *Ann. Glaciol.,* **25,** 282–286.
Janjić, Z. I., 1994: The step-mountain eta coordinate model: Further developments of the convection, viscous sublayer, and turbulence closure schemes. *Mon. Wea. Rev.,* **122,** 927–945.
Kiehl, J. T., J. J. Hack, G. B. Bonan, B. A. Boville, B. P. Briegleb, D. L. Williamson, and P. J. Rasch, 1996: Description of the NCAR community climate model (CCM3). NCAR Tech. Note NCAR/TN-420+STR, 152 pp.
Manning, K. W., and C. A. Davis, 1997: Verification and sensitivity experiments for the WISP94 MM5 forecasts. *Wea. Forecasting,* **12,** 719–735.
Meyers, M. P., P. J. DeMott, and W. R. Cotton, 1992: New primary ice-nucleation parameterizations in an explicit cloud model. *J. Appl. Meteor.,* **31,** 708–721.
Oerlemans, J., and H. Vugts, 1993: A meterological experiment in the ablation zone of the Greenland ice sheet. *Bull. Amer. Meteor. Soc.,* **74,** 355–365.
Parish, T. R., 1984: A numerical study of strong katabatic winds over Antarctica. *Mon. Wea. Rev.,* **112,** 545–554.
Pettré, P., M. F. Renaud, R. Renaud, M. Déqué, S. Planton, and J. C. André, 1990: Study of the influence of katabatic flows on the Antarctic circulation using GCM simulations. *Meteor. Atmos. Phys.,* **43,** 187–195.
Pinto, J. O., J. A. Curry, A. H. Lynch, and P. O. G. Persson, 1999: Modeling clouds and radiation for the November 1997 period of SHEBA using a column climate model. *J. Geophys. Res.,* **104,** 6661–6678.
Reisner, J., R. M. Rasmussen, and R. T. Bruintjes, 1998: Explicit forecasting of supercooled liquid water in winter storms using the MM5 mesoscale model. *Quart. J. Roy. Meteor. Soc.,* **124,** 1071–1107.
Steffen, K., J. E. Box, and W. Abdalati, 1996: Greenland Climate Network: GC-NET. *Special Report on Glaciers, Ice Sheets and Volcanoes, Tribute to M. Meier,* S. C. Colbeck, Ed., CRREL Special Report 96-27, 98–103.
van Lipzig, N. P. M., E. van Meijgaard, and J. Oerlemans, 1999: Evaluation of a regional atmospheric model using measurements of surface heat exchange processes from a site in Antarctica. *Mon. Wea. Rev.,* **127,** 1994–2011.
Walsh, K., and J. L. McGregor, 1996: Simulations of Antarctic climate using a limited area model. *J. Geophys. Res.,* **101,** 19 093–19 108.
Yen, Y. C., 1981: Review of thermal properties of snow, ice and sea ice. CRREL Rep. 81-10, 27 pp.